Lattice Dynamics and Thermal Expansion of Thulium

R. Ramji Rao and A. Rajput

Department of Physics, Indian Institute of Technology, Madras-600036, India

Z. Naturforsch. **34a**, 200–206 (1979); received August 24, 1978

The lattice dynamics, lattice specific heat and thermal expansion of the rare-earth metal thulium are worked out applying a model based on Keating's method. A frequency distribution function involving 50,880 frequencies has been employed. Using the calculated lattice heat capacity, the experimental C_p data of thulium are analysed to get the magnetic contribution to the specific heat in this metal. The energy of magnetic ordering and the magnetic entropy increase involved in the transition from the ordered antiferromagnetic phase to the disordered paramagnetic phase are evaluated. The lattice parameters and volume of thulium are also calculated as a function of hydrostatic pressure and compared with the experimental results.

1. Introduction

Thulium is a heavy rare-earth metal with an axial ratio of 1.579. The specific heat of Tm was measured by Jennings et al. [1] in the temperature range 0 to 360 K. Perez Albuerne et al. [2] determined experimentally the variation of the lattice parameters and volume of Tm with hydrostatic pressure upto 190 kbars. Srinivasan and Ramji Rao [3] proposed a model for the lattice dynamics, third-order elastic (TOE) constants and thermal expansion of hcp metals based on Keating's approach [4] and applied the same to magnesium, zinc and beryllium. In the present paper, this model is utilized to investigate the lattice dynamics, lattice heat capacity, TOE constants and the temperature variation of the effective Grüneisen functions for Tm. The energy of ordering W and the entropy change associated with the magnetic phase transition in Tm are calculated respectively from the magnetic specific heat and the magnetic entropy curves obtained by analysing the experimental C_p data [1] of Tm and using the calculated C_v[1]. The pressure variation of the lattice parameters and volume are also investigated for this metal.

The essence of Keating's method lies in the fact that the potential energy of the lattice is expressed in terms of the powers of the changes in the scalar products of the interatomic vectors so that it is automatically invariant towards rigid translations and rotations of the lattice. The two- and three-body interactions are taken into account in writing the potential energy, and the third-order parameters are incorporated in order to calculate the anharmonic properties of the crystal. The basis vectors and position coordinates of the sets of neighbours of the $\binom{0}{1}$ atom at the origin are given in Reference [3].

Reprint requests to Dr. R. Ramji Rao, Physics Department Indian Institute of Technology, Madras-600036, India.

0340-4811 / 79 / 0200-0200 $ 01.00/0

2. Lattice Dynamics

The experimental limiting frequencies at the zone centre and zone boundaries (Γ, A, M) in the symmetry directions (0001) and (01$\bar{1}$0), and the room temperature second-order elastic (SOE) constants are to be used in evaluating the twelve second-order parameters of the model. Neither the experimental dispersion relations nor the SOE constants of Tm have so far been reported in the literature. The limiting frequencies of Tm have, therefore, been obtained by extrapolating the appropriate experimental frequencies of Tb [5] and Ho [6] against the atomic number. The room

Table 1. The room-temperature SOE constants in 10^{11} dyn/cm^2. The SOE constants of Er and Lu are experimental [7, 8], while those of Tm are interpolated ones.

Metal	C_{11}	C_{33}	C_{12}	C_{13}	C_{44}
Er	8.63	8.55	3.05	2.27	2.81
Tm	8.63	8.40	3.10	2.45	2.77
Lu	8.623	8.086	3.20	2.80	2.679

Table 2. Frequencies ω in 10^{13} Hz. The frequencies of Tb and Ho are experimental [5, 6] and those of Tm are extrapolated values.

	[0001] direction		[01$\bar{1}$0] direction	
Metal	LO(Γ_3^+)	TO(Γ_6^-)	TO(Z) (M_3^+)	TA(Z) (M_4^-)
Tb	2.042	1.144	1.816	1.100
Ho	2.136	1.219	1.916	1.232
Tm	2.230	1.294	2.016	1.364

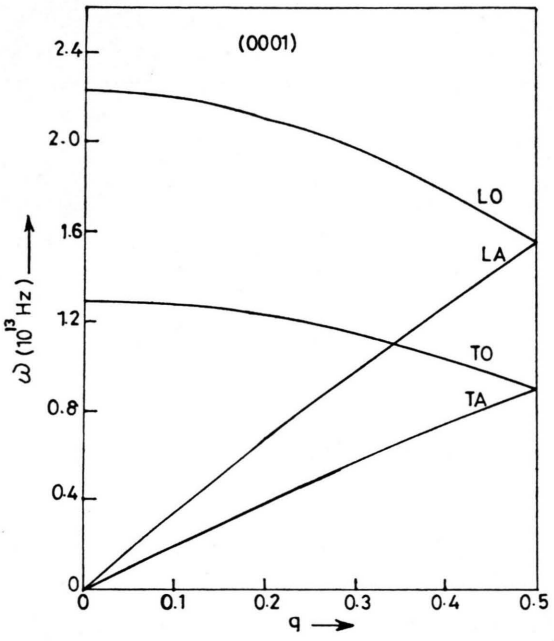

Fig. 1a. Theoretical phonon dispersion curves of Tm in the symmetry direction [0001].

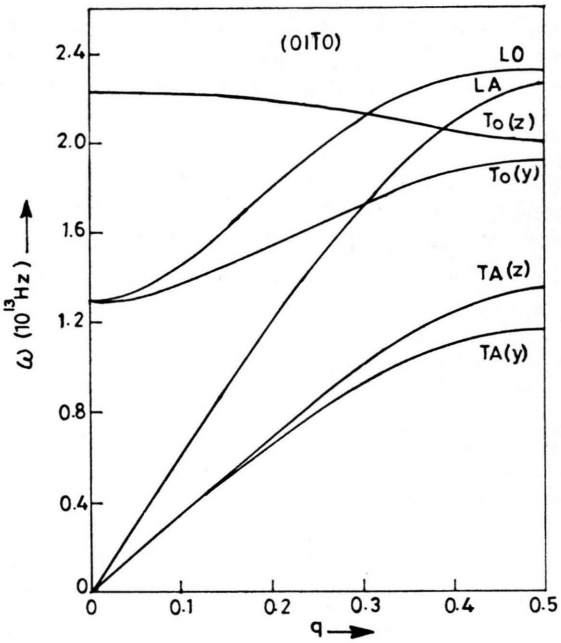

Fig. 1b. Theoretical phonon dispersion curves of Tm in the symmetry direction [01$\bar{1}$0].

Second order parameters	Value in 10^{11} dyn/cm^2
$(D^4/Va)\alpha$	0.861
$(D^4/Va)\tau$	0.392
$(D^4/Va)\gamma$	1.453
$(D^4/Va)\sigma$	− 0.079
$(D^4/Va)\beta$	0.175
$(D^4/Va)\varepsilon$	0.153
$(D^4/Va)\varkappa$	0.103
$(D^4/Va)\delta$	− 0.717

Table 3. Values of the second-order parameters for Tm in the present model.

temperature SOE constants of Tm are obtained by interpolating the room-temperature experimental SOE constants of Er [7] and Lu [8] against the atomic number. The interpolated SOE constants (Table 1) and four extrapolated frequencies (Table 2) of Tm have been used to fit the eight second-order parameters presented in Table 3. The theoretical dispersion curves of Tm in the (0001) and (01$\bar{1}$0) directions on the present model are shown in Figure 1.

3. Lattice Heat Capacity and Determination of the Magnetic Specific Heat and Magnetic Entropy Curves

The normalized frequency distribution function $g(\omega)$ for Tm shown in Fig. 2 is obtained by the root-sampling technique. The normal mode frequencies have been determined by solving the secular equation for different wave vectors $\boldsymbol{q}$ employing a program written for the computer IBM 370/155. The grid chosen for the wave vectors consists of 484 evenly spaced points in the irreducible volume of the Brillouin zone, this being equivalent to 8480 points in the entire volume of the Brillouin zone. The low frequency part of $g(\omega)$

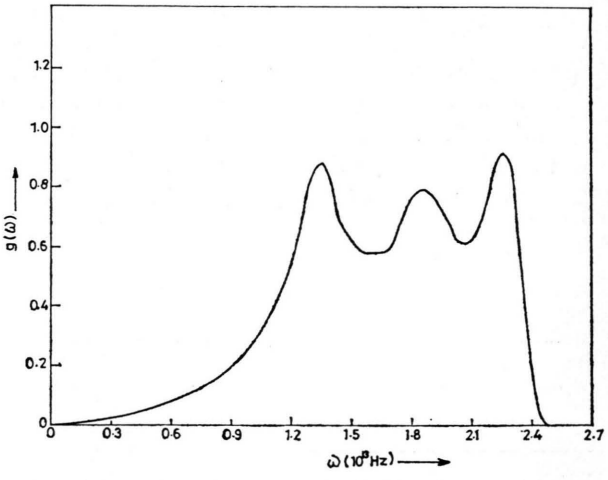

Fig. 2. Normalized frequency distribution function for Tm.

which does not contain sufficient number of frequencies, is drawn by using the relation $g(\omega) = C\omega^2$, the constant C being determined from the average value of $\sum_{j=1}^{3} V_j^{-3}(\theta, \varphi)$ over all directions. Here $V_j(\theta, \varphi)$ is the acoustic velocity of the jth mode of propagation in the direction (θ, φ).

The frequency distribution function of Fig. 2 is utilized to calculate the lattice specific heat as a function of temperature

$$C_v^{\mathrm{l}}(T) = \frac{3R\sum g(\omega)\,\sigma(\omega, T)}{\sum g(\omega)} \tag{3.1}$$

where $\sigma(\omega, T)$ is the Einstein specific heat function and R is the gas constant. Now the total specific heat at constant pressure is

$$C_p = C_v^{\mathrm{l}} + C_v^{\mathrm{e}} + C_v^{\mathrm{m}} + \delta C\,, \tag{3.2}$$

where C_v^{l}, C_v^{e} and C_v^{m} are respectively the lattice, electronic and magnetic contributions to the specific heat, and δC is the dilation term, given by

$$\delta C = A\,C_p^2\,T\,. \tag{3.3}$$

The electronic part of the specific heat is

$$C_v^{\mathrm{e}} = \gamma\,T\,. \tag{3.4}$$

The quantity "A" in Eq. (3.3) is practically independent of temperature and has the value 0.6582×10^{-5} mole cal^{-1} for Tm as has been quoted by Gschneidner [9]. The electronic specific heat constant γ in Eq. (3.4) is taken to be equal to 25.1×10^{-4} cal mole^{-1} K^{-2} for Tm. This is the average of the γ values of the four rare-earth metals La, Lu, Sc and Y reported by Lounasmaa and Sundström [10]. Using equations (3.1), (3.3) and (3.4) and the C_p data of Jennings et al. [1], the magnetic specific heat C_v^{m} is determined from Equation (3.2). The magnetic specific heat curve as well as the magnetic entropy curve for Tm are presented in Figure 3. This type of analysis was earlier done for Tb and Gd by Jennings et al. [11] and Hofmann et al. [12] respectively. The energy of magnetic ordering W and the magnetic entropy increase Smag involved in the transition from the magnetically ordered state at $T < Tc$ to one of disorder at $T > Tc$ are obtained respectively from the areas under the C_v^{m} vs. T curve and the C_v^{m}/T vs. T curve presented in Figure 3. The values of W and S_{mag} are reported in Table 4, and the latter is compared with that obtained from the theoretical expression $R\ln(2J+1)$ where the spin J has the value 6 for Tm.

Table 4. Results of separation of magnetic specific heat for Tm.

W (cal/mole)	Magnetic entropy S_{mag} (cal/mole K)	
	Experimental (from the present analysis)	Theoretical (from $R\ln(2J+1)$)
223	5.22	5.10

4. TOE Constants and Pressure Derivatives of SOE Constants

The model of Srinivasan and Ramji Rao [3] contains five third-order anharmonic parameters that enter into the theoretical expressions for the pressure derivatives of the SOE constants of a hcp crystal through its TOE constants, as was shown by Ramji Rao and Srinivasan [13]. The ten TOE constants of Tm have been calculated using two anharmonic parameters ξ and ζ, implying that anharmonic interactions upto second neighbours only are taken into account. These parameters correspond respectively to the J and I atoms, the first two neighbours of the $\binom{0}{1}$ atom at the origin. The J and I atoms in Tm being practically at the same distance from the $\binom{0}{1}$ atom, the parameters ξ and ζ have been taken equal and are so chosen as to give a consistently good fit of the experimental data on volume compression [2] for Tm to Murnaghan's equation [14] for V/V_0 (which involves the pressure derivatives of the SOE constants) at all pressures, the fitting being good within 0.8 percent at the highest pressure, viz., 106 kbars.

The values of ξ and ζ, the calculated TOE constants and the pressure derivatives of the SOE constants of Tm are shown in Table 5.

5. Thermal Expansion

a) Low-temperature Limit of Thermal Expansion

The low-temperature thermal expansion of a uniaxial crystal can be calculated knowing the generalized Grüneisen parameters (GPs) of the

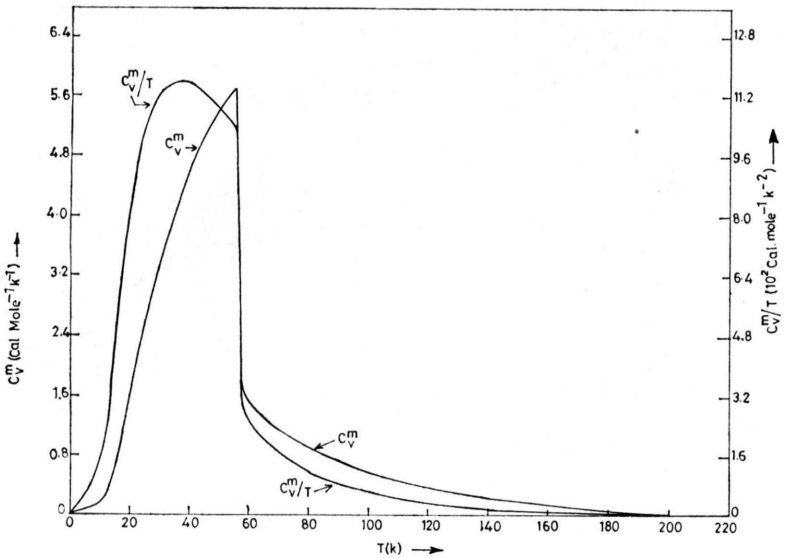

Fig. 3. The magnetic specific heat and magnetic entropy curves for Tm obtained from the present analysis.

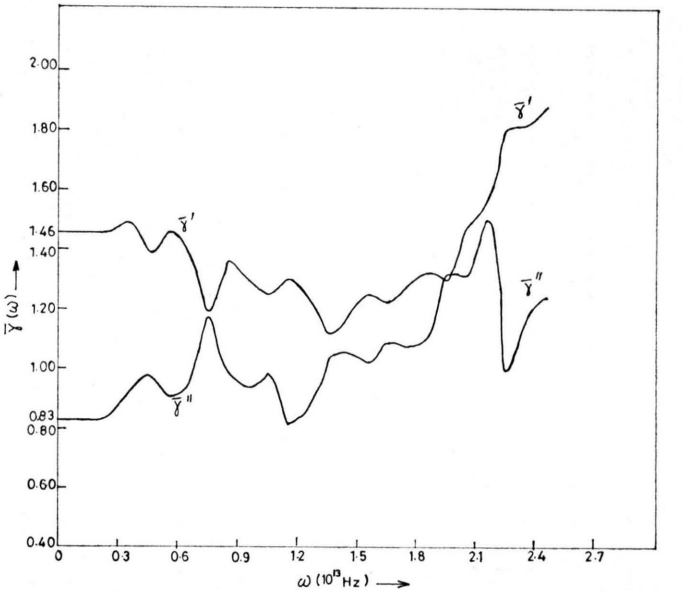

Fig. 4. $\bar{\gamma}'(\omega)$ and $\bar{\gamma}''(\omega)$ versus ω for Tm.

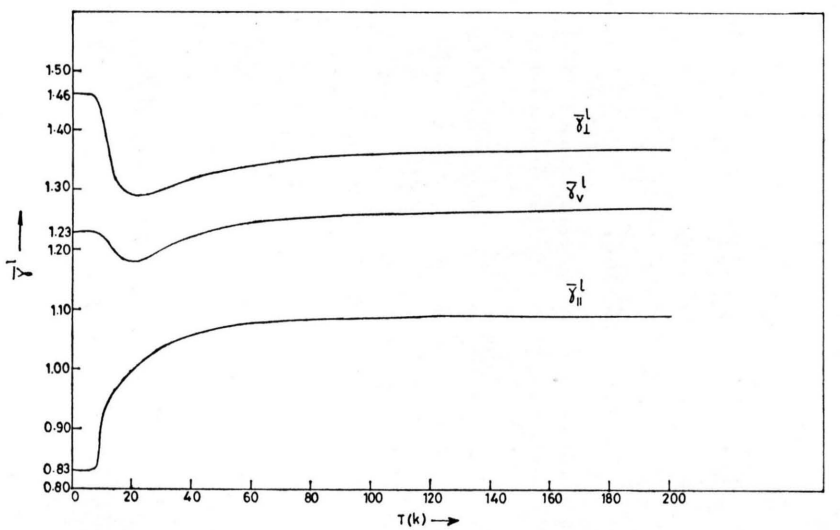

Fig. 5. $\bar{\gamma}_\perp{}^l(T)$, $\bar{\gamma}_\parallel{}^l(T)$ and $\bar{\gamma}_v{}^l(T)$ versus T for Tm.

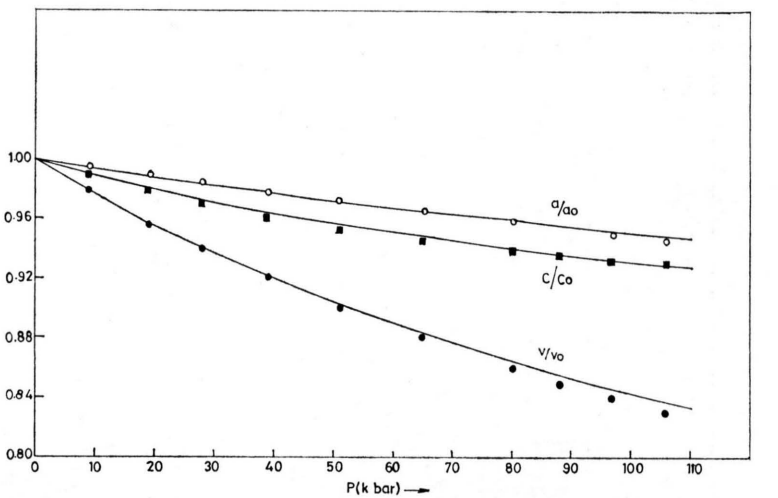

Fig. 6. Variation of a/a_0, c/c_0 and V/V_0 of Tm with hydrostatic pressure. The experimental values [2] of a/a_0, c/c_0 and V/V_0 are respectively denoted by open circles, closed squares and closed circles.

Table 5. Values of the third-order parameters, the TOE constants and the pressure derivatives of the SOE constants of Tm.

Third order parameters	Value in 10^{11} dyn/cm^2	TOE constants	Value in 10^{11} dyn/cm^2	Pressure derivatives of SOE constants	
				dC_{ij}/dp	Calculated values
$(D^6/Va)\,\xi$	− 7.370	C_{111}	− 99.41		
$(D^6/Va)\,\zeta$	− 7.370	C_{112}	− 35.45	dC_{11}/dp	6.92
		C_{113}	− 1.91		
		C_{123}	− 10.35	dC_{12}/dp	3.98
		C_{133}	− 22.91		
		C_{144}	− 7.97	dC_{33}/dp	7.08
		C_{155}	− 4.29		
		C_{222}	−121.72	dC_{44}/dp	1.43
		C_{333}	− 85.67		
		C_{344}	− 22.91	dC_{13}/dp	2.46

elastic wave propagating in the crystal. The GPs of the normal mode frequencies are defined as

$$\gamma'(\omega) = -\,\partial \ln \omega/\partial\varepsilon'; \qquad \gamma''(\omega) = -\,\partial \ln \omega/\partial\varepsilon'', \tag{5.1}$$

where ε' is a uniform areal strain in the basal plane and ε'' is a uniform longitudinal strain parallel to the unique axis. The effective Grüneisen functions $\overline{\gamma}_\perp{}^1(T)$ and $\overline{\gamma}_\parallel{}^1(T)$ are, by definition, the weighted averages of the GPs, and can be used to describe the temperature dependence of the linear expansion coefficients $\alpha_\perp$ and $\alpha_\parallel$ as follows:

$$\begin{aligned} V\alpha_\perp &= [(S_{11}+S_{12})\,\overline{\gamma}_\perp{}^1(T) + S_{13}\,\overline{\gamma}_\parallel{}^1(T)]\,C_v \\ &= \overline{\gamma}_\perp{}^{\mathrm{Br}}(T)\,C_v\,\chi_{\mathrm{iso}}, \\ V\alpha_\parallel &= [2S_{13}\,\overline{\gamma}_\perp{}^1(T) + S_{33}\,\overline{\gamma}_\parallel{}^1(T)]\,C_v \\ &= \overline{\gamma}_\parallel{}^{\mathrm{Br}}(T)\,C_v\,\chi_{\mathrm{iso}}, \end{aligned} \tag{5.2}$$

where S_{ij} are the elastic compliance coefficients, V is the molar volume and χ_{iso} is the isothermal compressibility. $\overline{\gamma}_\perp{}^{\mathrm{Br}}$ and $\overline{\gamma}_\parallel{}^{\mathrm{Br}}$ are the average Grüneisen functions used by Brugger and Fritz [15]. At very low temperatures, the acoustic modes are predominant and $\overline{\gamma}_\perp{}^1(T)$ and $\overline{\gamma}_\parallel{}^1(T)$ approach the limits conventionally designated by $\overline{\gamma}_\perp{}^1(-3)$ and $\overline{\gamma}_\parallel{}^1(-3)$ respectively. These limits are

$$\overline{\gamma}_\perp{}^1(-3) = \frac{\sum_{j=1}^{3}\int \gamma_j'(\theta,\varphi)\,V_j^{-3}(\theta,\varphi)\,d\Omega}{\sum_{j=1}^{3}\int V_j^{-3}(\theta,\varphi)\,d\Omega},$$

$$\overline{\gamma}_\parallel{}^1(-3) = \frac{\sum_{j=1}^{3}\int \gamma_j''(\theta,\varphi)\,V_j^{-3}(\theta,\varphi)\,d\Omega}{\sum_{j=1}^{3}\int V_j^{-3}(\theta,\varphi)\,d\Omega}. \tag{5.3}$$

Here $V_j(\theta,\varphi)$ is the wave velocity of the acoustic mode of polarization index j propagating in the direction (θ,φ); $\gamma_j'(\theta,\varphi)$ and $\gamma_j''(\theta,\varphi)$ are the GPs for the acoustic mode. The calculational procedure adopted here is that due to Ramji Rao and Srinivasan [16]. The calculated values of $\overline{\gamma}_\perp{}^1(-3)$ and $\overline{\gamma}_\parallel{}^1(-3)$ for Tm turn out to be 1.46 and 0.83 respectively. The low-temperature limit of the lattice volume thermal expansion is given by

$$\overline{\gamma}_L = 2\,\overline{\gamma}_\perp{}^{\mathrm{Br}}(-3) + \overline{\gamma}_\parallel{}^{\mathrm{Br}}(-3) \tag{5.4}$$

and its value for Tm is found to be 1.23.

b) Temperature Dependence of Effective Grüneisen functions

The procedure of Blackman [17] has been followed in calculating the temperature dependence of the effective Grüneisen functions $\overline{\gamma}_\perp{}^1(T)$ and $\overline{\gamma}_\parallel{}^1(T)$. The normal mode frequencies $\omega(\boldsymbol{q}, j)$ and the GPs $\gamma'(\boldsymbol{q}, j)$ and $\gamma''(\boldsymbol{q}, j)$ have been obtained for 484 points evenly distributed over 1/24th of the volume of the Brillouin zone using a program written for the computer IBM 370/155. The individual GPs γ' and γ'' for the various normal mode frequencies in each frequency interval of width $\Delta\omega = 0.1 \times 10^{13}$ Hz are noted and the average values $\overline{\gamma}'$ and $\overline{\gamma}''$ of these GPs are found for each interval. Figure 4 shows the plots of $\overline{\gamma}'$ and $\overline{\gamma}''$ versus ω, their low-frequency values tending to their respective low-temperature limits 1.46 and 0.83. The following equations are then used to yield $\overline{\gamma}_\perp{}^1(T)$ and $\overline{\gamma}_\parallel{}^1(T)$:

$$\overline{\gamma}_\perp{}^1(T) = \frac{\int_0^{\omega_{\max}} \overline{\gamma}'(\omega)\,g(\omega)\,\sigma(\omega,T)\,d\omega}{\int_0^{\omega_{\max}} g(\omega)\,\sigma(\omega,T)\,d\omega},$$

$$\bar{\gamma}_{\parallel}^{\,1}(T) = \frac{\int_0^{\omega_{\max}} \bar{\gamma}''(\omega)\, g(\omega)\, \sigma(\omega, T)\, \mathrm{d}\omega}{\int_0^{\omega_{\max}} g(\omega)\, \sigma(\omega, T)\, \mathrm{d}\omega} . \quad (5.5)$$

The Grüneisen functions $\bar{\gamma}_{\perp}^{\,\mathrm{Br}}(T)$ and $\bar{\gamma}_{\parallel}^{\,\mathrm{Br}}(T)$ are then obtained from Eqs. (5.2) and used to determine the volume Grüneisen function from

$$\bar{\gamma}_v^{\,1}(T) = 2\bar{\gamma}_{\perp}^{\,\mathrm{Br}}(T) + \bar{\gamma}_{\parallel}^{\,\mathrm{Br}}(T) . \quad (5.6)$$

The temperature variation of $\bar{\gamma}_{\perp}^{\,1}(T)$, $\bar{\gamma}_{\parallel}^{\,1}(T)$ and $\bar{\gamma}_v^{\,1}(T)$ is shown in Figure 5. The high-temperature limit of $\bar{\gamma}_v^{\,1}(T)$ i.e., $\bar{\gamma}_H$ works out to 1.27. This compares well with the value 1.38 obtained by Gschneidner [9] from the experimental thermal expansion and $C_v^{\,1}$ data of Tm. However, if the value of γ is taken to be that given by Lounasmaa and Sundström [10] instead of the much higher value ($= 47.1 \times 10^{-4}$ cal mole^{-1} K^{-2}) used by Gschneidner [9] for computing the experimental $C_v^{\,1}$ of Tm, we get the value 1.22 for $\bar{\gamma}_H$ of Tm, which is very close to our calculated value of 1.27.

6. Variation of Lattice Parameters with Hydrostatic Pressure

Thurston's extrapolation formulae [18] and the theoretical TOE constants of Tm have been made use of for investigating the pressure variation of the lattice parameters in this metal. For the principal stretches λ_i ($i = 1, 2, 3$), Thurston's extrapolation formula reads

$$\lambda_i = \left[\left(\frac{B}{B_0}\right)^{-B_0^2 Y_{i0}/(B_0')^2}\right] \cdot \exp\{(a_i + B_0\, Y_{i0}/B_0')\, P\} \quad (6.1)$$

which is consistent with a linear pressure dependence of the bulk modulus. For a hexagonal crystal $\lambda_1 = \lambda_2 = \lambda_{\perp}$ and $\lambda_3 = \lambda_{\parallel}$ so that Eq. (6.1) becomes respectively

$$\lambda_{\perp} = a/a_0 = \left[\left(\frac{B}{B_0}\right)^{-B_0^2 Y_{\perp 0}/(B_0')^2}\right] \cdot \exp\{(a_{\perp} + B_0\, Y_{\perp 0}/B_0')\, P\} ,$$

$$\lambda_{\parallel} = c/c_0 = \left[\left(\frac{B}{B_0}\right)^{-B_0^2 Y_{\parallel 0}/(B_0')^2}\right] \cdot \exp\{(a_{\parallel} + B_0\, Y_{\parallel 0}/B_0')\, P\} . \quad (6.2)$$

Here (a_0, c_0) and (a, c) are the lattice parameters at pressures zero and "P" respectively. B is the bulk modulus at pressure "P"; B_0 and B_0' are the bulk modulus and its pressure derivative at zero pressure. The expressions for the parameters in Eqs. (6.2) are given in Thurston's paper [18]. From Eqs. (6.2), the volume ratio is

$$V/V_0 = (\lambda_{\perp})^2\, \lambda_{\parallel} = \left(1 + P\,\frac{B_0'}{B_0}\right)^{-1/B_0'} . \quad (6.3)$$

This is the same as Murnaghan's equation [14] mentioned in Sect. 4 of this paper. In Fig. 6, the theoretical results for a/a_0 and c/c_0 are compared with the corresponding experimental data [2] at various pressures upto 106 kbars beyond which Tm does not retain its hcp structure. Very good agreement is found between theory and experiment, the maximum discrepancy in case of either a/a_0 or c/c_0 being only 0.4 percent. The calculated values of $a_{\perp}$, $a_{\parallel}$, $Y_{\perp 0}$, $Y_{\parallel 0}$ and those of B_0 and B_0' for Tm are noted below.

$$\begin{aligned} a_{\perp} &= -0.688\ \text{mbar}^{-1}, \\ a_{\parallel} &= -1.145\ \text{mbar}^{-1}; \\ Y_{\perp 0} &= 6.425\ \text{mbar}^{-2}, \\ Y_{\parallel 0} &= 14.488\ \text{mbar}^{-2}; \\ B_0 &= 0.397\ \text{mbar}, \quad B_0' = 4.300 . \end{aligned}$$

7. Discussion

The general pattern of the phonon dispersion curves of Tm (Fig. 1) is similar to those of other hcp metals. The magnitudes of the TOE constants C_{111}, C_{222} and C_{333} are small, which is true for other rare-earth metals like Ho [19]. The GPs γ' and γ'' in Tm have relatively small values, another characteristic of the rare-earth metals. The high-temperature limit of the volume lattice thermal expansion agrees very well with that estimated from the experimental data on thermal expansion and specific heat of Tm. The calculated changes of a/a_0 and c/c_0 with hydrostatic pressure are in excellent agreement with the experimental data of Perez Albuerne et al. [2]. We are thus led to the expectation that any future experimental measurements of the TOE constants of Tm would show comparable agreement with our calculated values. Further we can make the inference that inclusion of anharmonic interactions upto second neighbours in Tm explains quite well the anharmonic properties of this metal studied in this paper. The good agreement between the magnetic entropy calculated from the C_v^{m}/T vs. T curve and that obtained from the formula $R \ln(2J+1)$ lends credibility to our

calculated C_v[1] values, which, in turn, implies that the normalized frequency distribution function of Tm obtained on the present model is sufficiently good to explain its thermal properties to a high degree of accuracy.

Acknowledgement

One of the authors (A.R.) expresses his gratefulness to the University Grants Commission, Government of India, for the award of a teacher fellowship.

[1] L. D. Jennings, E. Hill, and F. H. Spedding, J. Chem. Phys. **34**, 2082 (1961).
[2] E. A. Perez-Albuerne, R. L. Clendenen, R. W. Lynch, and D. H. Drickamer, Phys. Rev. **142**, 392 (1966).
[3] R. Srinivasan and R. Ramji Rao, J. Phys. Chem. Sol. **32**, 1796 (1971); **33**, 491 (1972).
[4] P. N. Keating, Phys. Rev. **145**, 637 (1966); **149**, 674 (1966).
[5] J. C. Glyden Houmann and R. M. Nicklow, Phys. Rev. **B 1**, 3943 (1970).
[6] R. M. Nicklow, N. Wakabayashi, and P. R. Vijayaraghavan, Phys. Rev. **B 3**, 1229 (1971).
[7] E. S. Fisher and D. Dever, Trans. Metall. Soc. AIME **239**, 48 (1967).
[8] J. J. Tonnies, K. A. Gschneidner Jr., and F. H. Spedding, J. Appl. Phys. **42**, 3275 (1971).
[9] K. A. Gschneidner Jr., in Solid State Physics, Vol. 16, F. Seitz and D. Turnbull (Eds.), Academic Press, New York 1964, p. 350—415.
[10] O. V. Lounasmaa and L. J. Sundström, Phys. Rev. **150**, 399 (1966).
[11] L. D. Jennings, R. M. Stanton, and F. H. Spedding, J. Chem. Phys. **27**, 909 (1957).
[12] J. A. Hofmann, A. Paskin, K. J. Tauer, and R. J. Weiss, J. Phys. Chem. Solids **1**, 45 (1956); **15**, 187 (1960).
[13] R. Ramji Rao and R. Srinivasan, Phys. Stat. Sol. **31**, K 39 (1969).
[14] F. D. Murnaghan, Proc. Nat. Acad. Sci. USA. **30**, 244 (1944).
[15] K. Brugger and T. C. Fritz, Phys. Rev. **157**, 524 (1967).
[16] R. Ramji Rao and R. Srinivasan, Phys. Stat. Sol. **29**, 865 (1968); Proc. Indian Natl. Sci. Acad. **36 A**, 97 (1970).
[17] M. Blackman, Proc. Phys. Soc. London **B 70**, 827 (1957).
[18] R. N. Thurston, J. Acoust. Soc. Amer. **41**, 1093 (1967).
[19] R. Ramji Rao and A. Ramanand, Phys. Stat. Sol. (a) **42**, 247 (1977).